JOURNAL OF SPACECRAFT AND ROCKETS
Vol. 37, No. 3, May–June 2000

Oxidation of Hypervelocity Impacted Reinforced Carbon–Carbon

Donald M. Curry* and Vuong T. Pham†
NASA Johnson Space Center, Houston, Texas 77058
and
Ignacio Norman‡ and Dennis C. Chao§
The Boeing Company, Houston, Texas 77058

Results from arcjet tests conducted at the NASA Johnson Space Center on reinforced carbon–carbon samples subjected to hypervelocity impact are presented. The test specimens are representative of reinforced carbon–carbon component used on the Space Shuttle Orbiter. The arcjet testing established the oxidation characteristics of reinforced carbon–carbon when hypervelocity projectiles, simulating meteoroid/orbital debris, impact the reinforced carbon–carbon material. In addition, analytical modeling of the increased material oxidation in the impacted area, using measured hole growth data, to develop correlations for use in trajectory simulations is discussed. Entry flight simulations are useful in assessing the increased Space Shuttle reinforced carbon–carbon component degradation as a result of impact damage and the hot gas flow through an enlarging hole into the wing leading-edge cavity.

Nomenclature

$\dot{D}_b$ = back coating hole diameter growth rate, in./s
$\dot{D}_f$ = front coating hole diameter growth rate, in./s
IE = impact energy, ft · lbf
P = pressure, lbf/ft^2
P_0 = atmospheric pressure (2116.2 lbf/ft^2)
$X1$ = function of pressure defined by Eq. (2)
$X2$ = function of impact energy defined by Eq. (3)
$X3$ = function of pressure defined by Eq. (5)
$X4$ = function of impact energy defined by Eq. (6)

Introduction

DURING the early flights of the Space Shuttle, micrometeoroids and orbital debris were not recognized as a significant hazard to the orbiters. However, more recent models of the space environment suggest that micrometeoroids and orbital debris (MOD) pose a significant threat to the orbital vehicles. The reinforced carbon–carbon (RCC) wing leading edge and nose cap are especially vulnerable to this MOD environment and have been identified as areas of the orbiter that appear to pose the highest risk for critical failure.

The RCC is a structural composite, and due to the brittle nature of the RCC silicon carbide coating and the requirement to maintain oxidation protection, the effect of impact damage on the mission life and structural performance of the RCC components is of concern. Impact damage may occur from a variety of threats with a wide range of impact speeds. Meteoroids and manufactured orbital debris represent a source of high-velocity impact damage, and other sources of damage include handling and service damage, launch debris, and runway debris from landing. Orbital debris can impact orbiting spacecraft at velocities from less than 3000 ft/s to over 46,000 ft/s and meteoroids from 33,000 ft/s to over 230,000 ft/s.

The effects of hypervelocity impact damage on the oxidation performance on the RCC material has been investigated experimentally. Hypervelocity impact testing produced complete penetration or through-holes in the test specimens. The arcjet tests were performed on RCC samples impacted at hypervelocity to establish the rate of enlargement of the through-holes due to oxidation. The hole growth rate was used to develop corrections for predicting the increased oxidation during a typical orbiter entry. The typical entry hole growth rates can be used to calculate the hot gas influx into the wing leading-edge cavity through the resulting burn-through hole and assess structural vehicle component damage. These hole growth correlations, along with the probabilities of impact damage, are used to assess MOD impacts on the orbiter RCC vehicle components for the establishment of flight rules and initial impact hole acceptability criteria. The objective of this paper is to describe these tests and present test results and correlations.

RCC Test Articles

Test articles consisted of silicon–carbide (SiC) coated RCC samples. Shown in Fig. 1 are the nominal dimensions of the coating and substrate that make up the 0.25-in.-thick RCC test samples. These samples are representative of RCC components on the Space Shuttle Orbiter, which include the nose cap, wing leading-edge panels, an area between the nose landing gear door and nose cap, and a small area surrounding the forward attach fitting of the external tank to the orbiter.

The test sample substrate is all carbon composite laminate fabricated in a multiple pyrolysis and densification process from a 19-ply phenolic graphite layup. The substrate has a density of 90–100 lb/ft^3 and is typically 0.17–0.21 in. thick.

The oxidation resistant SiC coating is formed in a diffusion reaction process. It is typically 0.02–0.04 in. thick. Further oxidation resistance is provided by impregnation with tetraethylorthosilicate (TEOS) that when cured leaves a silicon dioxide (SiO_2) residue throughout the coating and substrate. Any surface porosity or microcracks are filled by an application of a surface sealant (sodium silicate/SiC mixture) in the final step of the fabrication process. More details on the development and fabrication of the orbiter RCC applications are given by Curry et al.[1] and Dotts et al.[2]

Hypervelocity Impact Tests

Hypervelocity impact (HVI) testing of RCC was conducted at the NASA Johnson Space Center (JSC) Hypervelocity Impact Technology Facility (HIT-F),[3] where 24 tests were conducted to investigate the effects of HVI of projectiles simulating MOD striking RCC.

Two types of targets were tested: 10 flat plate 6 × 6 in. RCC target samples and a curved surface sample were used for pretesting, and a full-scale RCC wing leading-edge panel was tested. All samples had a thickness of approximately 0.25 in.

The primary objective of these tests was to impact each sample twice, each impact producing a separate and complete penetration. Impact holes of 0.125, 0.25, or 0.375 in. diameter were produced. The samples had to be impacted in the HIT-F such that two circular disks measuring 2.8 in. in diameter, with the impact hole in the

Presented as Paper 99-3461 at the AIAA 33rd Thermophysics Conference, Norfolk, VA, 28 June–1 July 1999; received 10 August 1999; revision received 26 January 2000; accepted for publication 2 February 2000.

*Aerospace Technologist, Structures and Mechanics Division. Member AIAA.
†Aerospace Technologist, Structures and Mechanics Division.
‡Engineer/Scientist, Reusable Space Systems Division.
§Engineer/Scientist, Reusable Space Systems Division. Member AIAA.

Table 1 Summary of reinforced carbon–carbon hypervelocity test results

JSC HIT-F sample identification	JSC HIT-F shot no.	Projectile diameter used,[a] in.	Projectile mass, mg	Projectile velocity, ft/s	Projectile kinetic energy, ft · lb	Through-hole damage hole size, in.	Front diameter of damage, in.	Back diameter of damage, in.
10.1	A3085	0.0781	12.39	21,195	190.69	0.354 × 0.354	0.867	1.035
9.1	A3086	0.0781	11.65	22,508	202.19	0.354 × 0.374	0.819	1.208
8.1	A3087	0.0781	11.53	21,753	186.92	0.374 × 0.354	0.92	1.083
7.1	A3088	0.0781	11.62	22,639	204.03	0.374 × 0.374	0.932	1.159
6.1	A3089	0.0781	11.70	23,033	212.64	0.354 × 0.374	0.888	1.18
4.1	A3093	0.0625	5.86	22,278	99.64	0.256 × 0.256	0.752	0.952
5.1	A3095	0.0625	5.68	23,098	103.82	0.256 × 0.276	0.776	0.962
3.1	A3096	0.0625	5.82	23,262	107.90	0.256 × 0.276	0.792	0.874
10.2	A3097	0.0625	5.67	22,803	101.01	0.256 × 0.256	0.756	0.966
9.2	A3098	0.0625	5.97	23,361	111.61	0.256 × 0.256	0.801	0.965
8.2	A3099	0.0492	2.81	23,361	52.54	0.138 × 0.138	0.673	0.701
7.2	A3100	0.0492	2.92	23,033	53.07	0.138 × 0.138	0.649	0.675
6.2	A3101	0.0492	2.85	23,295	52.98	0.158 × 0.158	0.685	0.725
4.2	A3105	0.0625	5.28	23,197	97.33	0.256 × 0.236	0.803	1.142
2.1	A3103	0.0625	5.71	23,000	103.48	0.256 × 0.236	0.777	0.968
3.2	A3108	0.0781	11.61	23,000	210.41	0.0374 × 0.354	0.913	1.069

[a]Projectile material Al2017-T4; projectile shape, sphere; all impact angles are 0 deg (normal to surface).

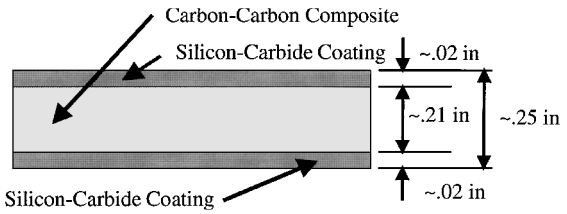

Fig. 1 RCC test article dimensions (typical).

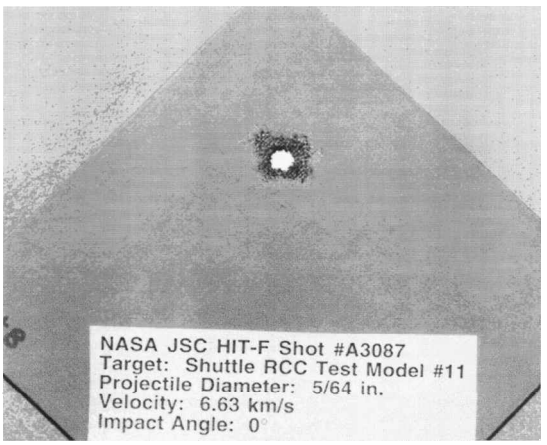

Fig. 2 Typical posttest photograph of hypervelocity impacted 6 × 6 in. RCC panel.

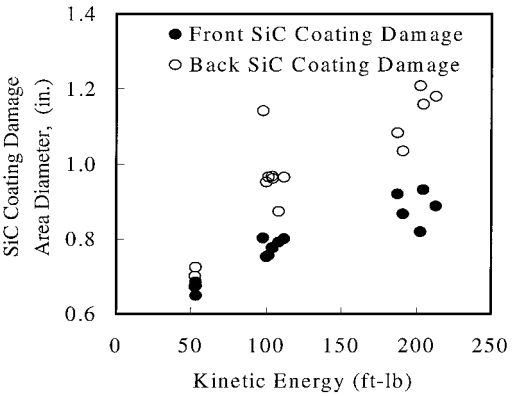

Fig. 3 Hypervelocity impact energy vs RCC coating damage area.

center, could be cut from each sample. This sample size was required to fit the specimen holders for arcjet testing. Data were collected in the HIT-F for correlation of projectile size to hole size. After each sample was tested in the HIT-F, that sample was sent to the JSC Arcjet Facility.

The objective for testing the full-scale wing leading-edge panel was to collect data for correlation of projectile size to the hole size through the top of the panel and the secondary damage that would occur to the bottom of the panel. There was interest in what kind of secondary damage would occur to the wing spar insulation inside the wing leading-edge panel. These results are not presented in this paper and are reported separately.[3]

Table 1 presents a summary of the impact test results, and a representative photograph of the target damage is shown in Fig. 2. Figure 2 shows the result of a $\frac{5}{64}$-in.-diam aluminum sphere impacting the 6 × 6 in. RCC sample at 21,850 ft/s normal to the surface. Because the SiC coating is brittle, the coating is damaged in an area around the impact site over 10 times larger than the projectile diameter. The hole through the specimen exposes the RCC substrate over an area four times larger than the projectile diameter. Figure 3 illustrates the approximate front and back coating damage diameter as a function of impact energy. The coating on the rear side of the RCC is damaged in a wide area, larger than the front. There is internal damage in the RCC substrate that can extend significantly beyond the external damage that is readily detected by visual observation. Internal damage in the RCC consists of microcracks and delaminations.

The hole diameters that were selected to be used for producing the arcjet test specimens were sizes of 0.125, 0.25, and 0.375 in., with kinetic energies of 50, 100, and 200 ft-lb, respectively.

Arcjet Testing

The objective of the arcjet testing was to establish the oxidation characteristics of RCC with HVI damage. RCC specimens were exposed to constant heating conditions for specific test points at temperatures of 2500 and 2800°F and pressures of 50–180 lbf/ft^2.

This test program was conducted in the JSC's Atmospheric Reentry Materials and Structures Evaluation Facility (ARMSEF). This facility simulates atmospheric entry conditions by heating test gas or gas mixtures electrically using a segmented, constricted, 10-MWDC arc heater. For this test program, the gas mixture was nitrogen and oxygen to simulate air. Once the air was heated to a high-energy (high-enthalpy) level inside the arc heater, it was then expanded supersonically through a conical nozzle, which has a 5 in. diameter at the exit plane. The high-enthalpy supersonic flowfield was formed and then captured by a downstream supersonic diffuser. Inside the chamber, a hydraulic model insertion system permits the test articles to be located outside the flowfield until the required test conditions have been established. Model insertion and retraction are normally performed within 1 s from the command signal, thereby producing a

step pulse heating profile on insertion and an immediate cessation of oxidation on retraction. During the test, the chamber static pressure was maintained below 7.73×10^{-3} lbf/in.^{2} by a four-stage steam ejector system.

The facility data acquisition system obtained facility and test article data at a rate of 10 Hz. Surface temperature was monitored by a 0.865-μm optical pyrometer aimed in such a way that the entire field of view was covered by the specimen in the area between the hole and the edge of the specimen. Once the hole starts to grow, the exposed and burning carbon substrate will affect the measurements. Because of the potential erroneous surface temperature feedback, the test runs were made with constant arc heater parameters as identified in the calibration runs.

Two super video home system video cameras were mounted outside on the test chamber. One was used to visually monitor and record the test articles' surfaces for transient hole diameter measurements. The other was used to monitor the flowfield and the overall interior of the test chamber.

The arcjet test specimens were fabricated from a 6×6 in. panel that was first impacted at the appropriate energy level to produce a desirable hole diameter. The sample was then cut (reduced) to approximately 2.8 in. diameter with the impacted hole at the center to make an arcjet test specimen. Test specimens were cut from an impacted panel using a high power CO_2 laser. One of the benefits from the laser cutting was the melted silicon carbide coating deposited on the exposed carbon edge, which acted as another oxidation protection layer. Once a specimen is cut from a panel, four small retention pin holes approximately $\frac{1}{8}$ in. in diameter and $\frac{1}{8}$ in. deep were drilled 90 deg apart on its carbon-exposed edge. The entire carbon-exposed edge was then repaired with a mixture of Sermabond 487 and 1000 grit silicon carbide powder that was cured by heating to 300°F in air.

The test specimen holder used during these tests is shown in Fig. 4. Figure 4 shows the 2.0-in.-diam hole, through which gases that are ingested through the impact holes can pass without restriction. Ceramic rods support the holder such that the flow may be smoothly diverted by a water-cooled conical interface block. The outlet slot between the holder and interface block has an area that is over 15 times the largest posttest impact hole area. Because the pressure just outside the slot is less than 0.6 lbf/ft^2, sonic conditions are maintained at the impact hole with large margin. In addition, a stagnation pressure measurement at the forward end of the conical flow diverter indicated that sonic conditions existed at the impact holes.

A view of one of the fixtures during the arcjet test is presented in Fig. 5. Figure 5 shows the normal shock in front of the specimen and the flow of ingested gases out the rear of the fixture. The arcjet nozzle, plasma flowfield glow, and the mirrors that are used to record the specimen face during testing are visible.

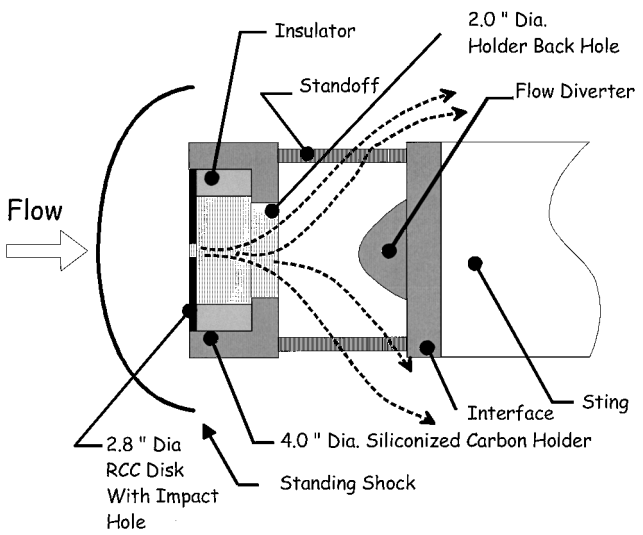

Fig. 4 Arcjet test specimen holder configuration.

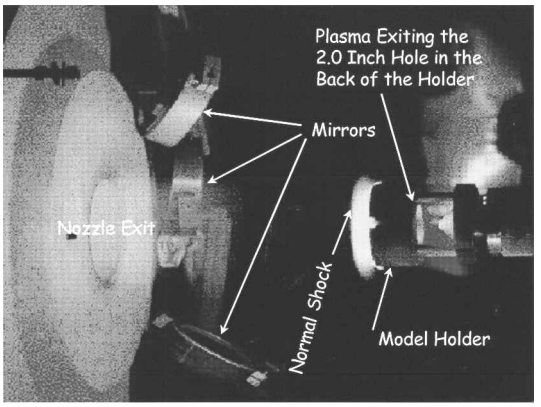

Fig. 5 Specimen in chamber during test.

Test conditions were established by measuring the temperature of an undamaged specimen with an optical pyrometer that repeatedly agreed to within 15°F with imbedded thermocouples in RCC calibration specimens (tested during many test programs over the last 5 years). The test specimens were exposed to constant heating conditions established with the undamaged specimens. No attempt was made to adjust to target temperatures because the presence of the impact damage was expected to change the temperature measurement. Facility operating parameters such as current, voltage, test gas flow rate, oxygen percentage, chamber pressure, arc column pressure, energy balance enthalpy, and gas injection manifold pressure were recorded during the calibration test and monitored for repeatability during subsequent tests. The arcjet test facility parameters used in this program were air mass-flow rate $\dot{m} = 0.2$–0.7 lbm/s, heater current, $I = 530$–1175 A, and bulk enthalpy $h = 2400$–7200 Btu/lbm.

A video camera mounted outside the chamber viewed each model indirectly through a window with the use of a small mirror mounted to one side of the exit nozzle of the plasma source. Because the models faced directly into the plasma flowfield, they were seen obliquely in the mirror, making the circular articles and the holder appear elliptically shaped. Video recording of the test specimen surface were made before, during, and after each test by viewing through a first surface mirror at an angle of approximately 45 deg. Posttest photographs with back lighting to emphasize the outlines of the penetration holes were taken for each test.

Specimen weights were taken to help assess substrate mass loss. Note that erosion of the substrate and the silicon carbide repair at the periphery and the erosion of silicon carbide coating near the impact hole could affect the interpretation of these data.

Results

Summarized in Table 2 are the results of 14 arcjet tests. Table 2 identifies the test conditions assigned to each specimen, impact energy sustained, the approximate level of visible pretest damage, arcjet exposure test time and conditions, and posttest arcjet dimensions of the hole growth.

Figures 6a and 6b present the front and back preexposure arcjet test photograph of NASA specimen 1159, a typical test specimen. Note from the photograph of the coating damage, as a result of the HVI and penetration, that the backside damage has a larger spalled coating area than the front-face coating spallation area. The NASA 1159 specimen was exposed to 2500°F at 50 lbf/ft^2 for 450 s.

Photographs of this typical posttest specimen, shown in Fig. 6, show the oxidation and growth of the impacted frontal area (Fig. 6c) and of the backside area (Fig. 6d) that occurred during the arcjet test. The hole growth of the test specimen grew by the oxidation of the exposed carbon–carbon substrate. Hole growth as a result of coating loss was not expected because there is negligible coating loss for temperatures between 2800 and 3000°F for the orbiter leading edge RCC.[4] Figure 6e presents an oblique view of NASA specimen 1159, where it can be seen that there was additional substrate loss that formed a dishing out of the carbon sandwiched between the SiC front and back coating.

Table 2 RCC orbital debris arcjet test program hole growth summary

JSC HIT-F sample identification	JSC arcjet identification	Targeted hole diameter, in.	Test conditions			Posttest measurements	
			Surface temperature, °F	Surface pressure, lb/ft^2	Test time, s	Front hole dimensions, in.	Back hole dimensions, in.
8.2	1161	0.125	2800	100	450	1.525–1.621	0.992–1.043
7.2	1166	0.125	2800	50	450	1.003–1.056	0.642–0.659
6.2	1165	0.125	2800	180	450	0.652–0.744	0.390–0.491
5.1	1157	0.250	2500	180	450	0.552–0.653	0.680–0.769
4.1	1151	0.250	2800	100	450	1.890–1.909	1.216–1.233
3.1	1158	0.250	2800	50	450	1.249–1.309	0.853–0.862
10.2	1160	0.250	2800	180	450	0.948–1.136	0.670–0.764
9.2	1159	0.250	2500	50	450	0.476–0.721	0.607–0.778
10.1	1145	0.375	2500	50	450	0.691–0.762	0.799–0.809
9.1	1144	0.375	2800	180	150	1.010–1.064	0.677–0.680
8.1	1143	0.375	2500	180	450	0.741–0.811	0.846–0.885
7.1	1142	0.375	2800	100	408	1.941–1.978	1.240–1.257
6.1	1152	0.375	2800	180	304	1.350–1.503	1.091–1.120
3.2	1172	0.375	2800	50	450	1.423–1.437	0.989–1.002

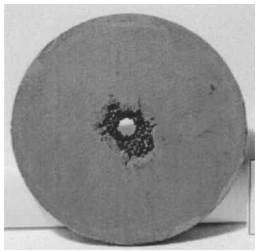

a) Frontside pre arcjet

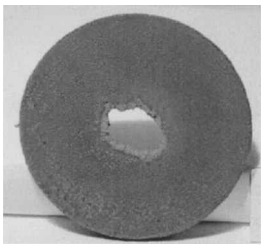

c) Frontside post arcjet

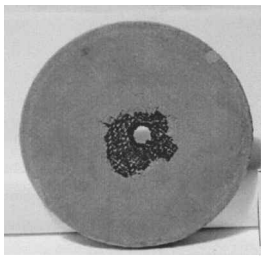

b) Backside pre arcjet

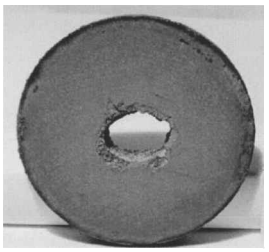

d) Backside post arcjet

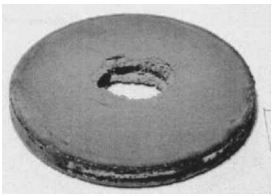

e) Post arcjet test oblique

Fig. 6 Hypervelocity impact damage pre and post arcjet test, 2500°F at 50 lbf/ft^2, model 1159.

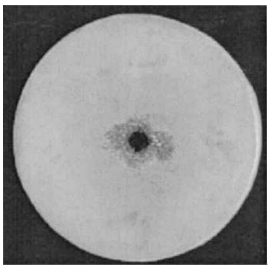

a) Frontside

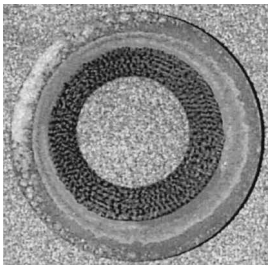

c) Frontside

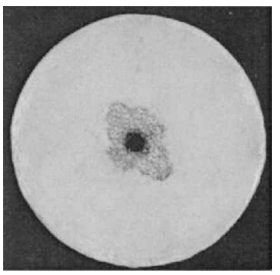

b) Backside

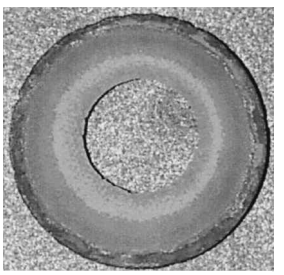

d) Backside

Fig. 7 NASA/JSC model 1151 pre- and post-arcjet exposure, 2800°F and 100 lbf/ft^2.

Figures 7a and 7b present the pre-arcjet exposure test photograph of NASA specimen 1151 that can be compared with the post-arcjet exposure photographs shown in Figs. 7c and 7d. For this test condition (2800°F and 100 lbf/ft^2) there was significant front-face coating erosion. In general, the front face of the damaged region grew faster than the backside of the specimen giving the hole a conical shape that is typical of all of the 2800°F tests.

An assessment of the hole growth was made by the JSC Image Science and Analysis Group (IS&AG) using videotapes of each test. Dimensional measurements of the diameters of both the larger front face of each hole (called the outer hole) and the back face of each hole (called the inner hole) were made for 14 of the tests. Figure 8 shows a photograph of a time cut that is typical for the videotape images used by the IS&AG to determine the inner and outer hole growth raw data. The minimum uncertainty in the diameter measurements is estimated to be 0.01 in. The minimum uncertainty applies only when

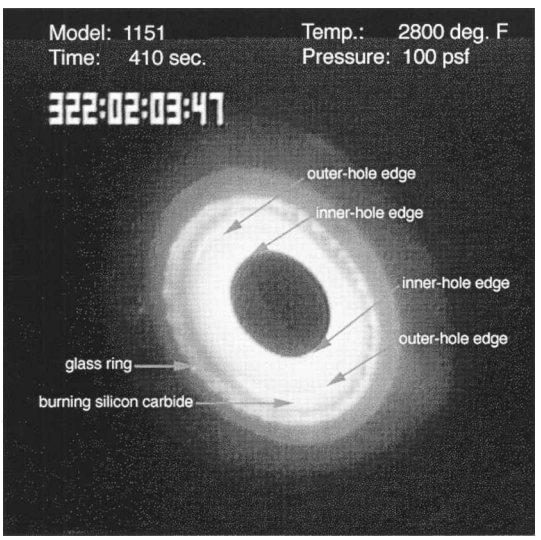

Fig. 8 Test photograph from the NASA/JSC IS&AG.

Table 3 Substrate mass loss of hypervelocity impacted RCC for the 2500°F tests

Test identification, JSC	Pressure, lb/ft^2	Impact energy, ft·lb	Damage hole diameter, in.	Ratio final hole growth[a]	Mass loss, test data, lbm	Mass loss, correlation,[b] lbm	Substrate mass loss ratio, test data/correlation
1145	50	190.69	0.375	2.0	5.50$E-$03	1.534$E-$03	3.59
1143	180	186.92	0.375	2.0	5.18$E-$03	2.722$E-$03	1.90
1159	50	111.61	0.25	2.4	4.84$E-$03	1.192$E-$03	4.06
1157	180	103.82	0.25	2.4	4.20$E-$03	2.00$E-$03	2.10

[a]Ratio final hole diameter/initial hole diameter.
[b]Correlation predictions considered the effective exposed substrate area of an impacted hole.

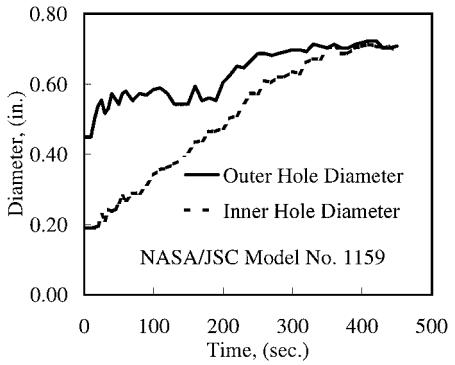

Fig. 9 Video hole growth data for a 2500°F, 0.25-in.-diam impacted hole.

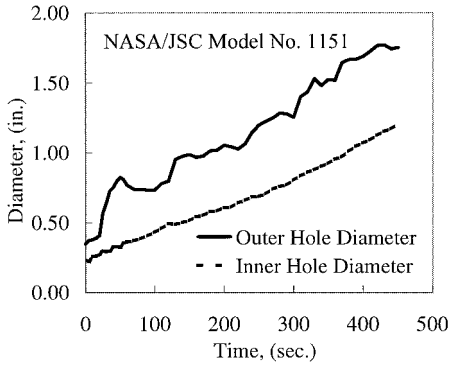

Fig. 10 Video hole growth data for a 2800°F, 0.25-in.-diam impacted hole.

the hole edge is well defined, focus is good, and there is no residual silicon carbide to interfere with the edge identification, generally true for the inner hole edge only. Outer edge uncertainty is 0.03–0.05 in. because of the appearance of new oxidizing (burning) rings of silicon carbide. As these new rings glow brightly their edges blur the image, giving a false image width.

Typical hole diameter measurements as a function of time made by the JSC IS&AG for the 14 tests articles are shown in Fig. 9 (2500°F) and Fig. 10 (2800°F).

Hole growths for the 2500°F tests showed only loss of the RCC substrate and no visible SiC coating loss. Thus, the 2500°F hole growth was circular on the exposed substrate with virtually no difference in the outer and inner diameter.

Hole growths of the 2800°F test specimens developed a conical shape, when viewed in cross section. The widest hole cone was formed by the 100-lbf/ft^2 test cases. The narrowest cone slopes were formed by the test cases tested at 180 lbf/ft^2. The conical hole shape phenomena is illustrated graphically in Fig. 11. The test data are grouped to show the conical shape (outer-ring diameter minus inner-ring diameter).

The hole growth data that was derived from the assessments of the videotapes of arcjet testing, the test measurements that were made at the hypervelocity lab, and the measurements performed at the ARMSEF were used for final hole growth prediction methods.

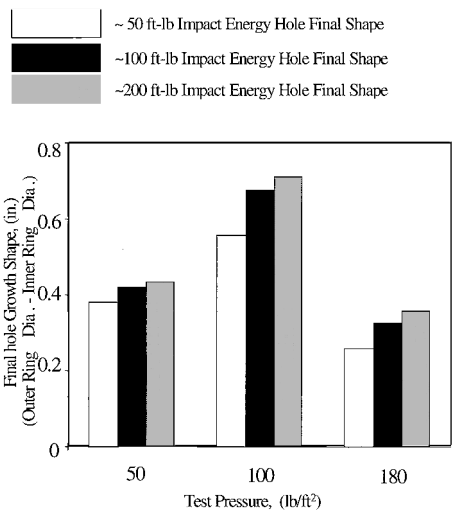

Fig. 11 Conical shape of hole growth at 2800°F.

Test Data Correlation and Application

2500°F Tests

The results of the data analysis for the 2500°F test data group are shown in Table 3. The results of the assessment of the 2500°F test specimens (Table 3) indicate that the substrate mass loss rate of an impacted RCC is about 2–4 times higher than the substrate mass loss for a nonimpacted noncoated RCC.[4] The 2500°F test results indicate that there is no coating oxidation for this temperature (Fig. 6); thus, the hole growth was limited to the size of the impact-damaged area.

2800°F Tests

The nominal Space Shuttle Orbiter multimission maximum temperature for RCC is 2800°F. Testing of RCC above the design limit has been previously performed, and the results of a RCC overtemperature test program suggest that at the temperature range from 2800 to 3080°F the RCC coating mass loss rate is nearly constant, and for temperatures below 2800°F the coating mass loss rate is negligible.[4] The coating hole growth rate correlation developed from the present test data treats the coating loss rate as a constant for the temperature range between 2800 and 3080°F.

Development of the correlations for the front and back coating hole growth rates were performed separately because they had different growth rates. The correlation assumed a constant hole growth rate with respect to time. A typical plot of the test data and the assumed constant hole growth rate are shown in Fig. 12.

Constant hole diameter growth rates, nine for the front coating hole and nine for the back coating hole, were established based on the test data of nine different test conditions. These growth rates, shown in Table 4, were developed from the video test data. With these growth rates, a two-stage, nonlinear regression analysis was performed. The first phase was to develop two single correlations. One was for the growth rate as a function of pressure ratio (test pressure divided by atmospheric pressure), and the other was for the growth rate as a function of the impact energy. These two correlations were then used as the second-generation independent variables, and a regression analysis was performed. The correlations for the front and back hole growth rates were developed separately

Table 4 Impacted RCC hole growth rate[a]

Impact energy, ft · lb	Pressure, lbf/ft^2	Hole diameter growth rate in./s
	Front coating hole[b]	
50	50	1.68E−03
50	100	3.04E−03
50	180	1.20E−03
100	50	1.98E−03
100	100	3.24E−03
100	180	1.80E−03
200	50	2.01E−03
200	100	3.20E−03
200	180	1.82E−03
	Back coating hole[b]	
50	50	1.36E−03
50	100	1.96E−03
50	180	1.18E−03
100	50	1.44E−03
100	100	2.18E−03
100	180	1.73E−03
200	50	1.64E−03
200	100	2.36E−03
200	180	1.93E−03

[a]Correlated from test data. [b]Temperature = 2800°F.

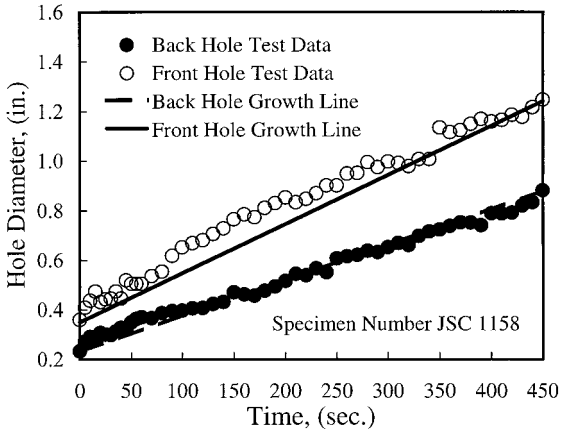

Fig. 12 Front and back hole growth rate comparison.

using the same procedure. The final correlations are shown hereafter.

The correlation for the front coating hole growth rate is

$$\dot{D}_f = -0.001684 + X1 + 0.795(X2) \quad (1)$$

where $\dot{D}_f$ is the front coating hole diameter growth rate in inches per second

$$X1 = -1.55(P/P_0)^2 + 0.164(P/P_0) - 1.11E-3 \quad (2)$$

$$X2 = 1.029E-3(\mathrm{IE})^{0.156} \quad (3)$$

The correlation for the back coating hole growth rate is

$$\dot{D}_b = -0.00165 + (X3) + 0.95(X4) \quad (4)$$

$$X3 = -7.056E-1(P/P_0)^2 + 7.9E-2(P/P_0) + 1.22E-5 \quad (5)$$

$$X4 = 6.50E-4(\mathrm{IE})^{0.21} \quad (6)$$

As the correlations indicate, the effect of the pressure environment on the hole growth rate is a second-order polynomial curve, and the effect of impact energy on the hole growth rate is a power curve. Shown in Figs. 13–16 are the comparisons between the test data and predictions, using the correlations, for both front and back coating hole growth rates. Details showing complete test data and correlations are given in Ref. 5.

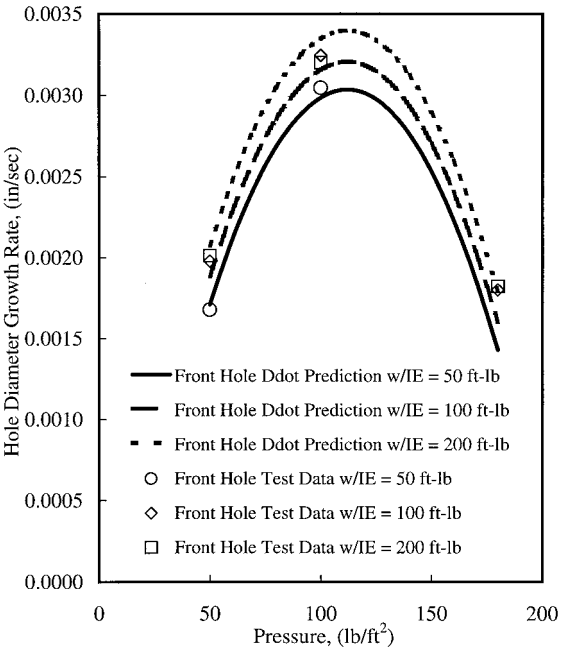

Fig. 13 Comparisons of test data and predictions for front hole growth rate (pressure).

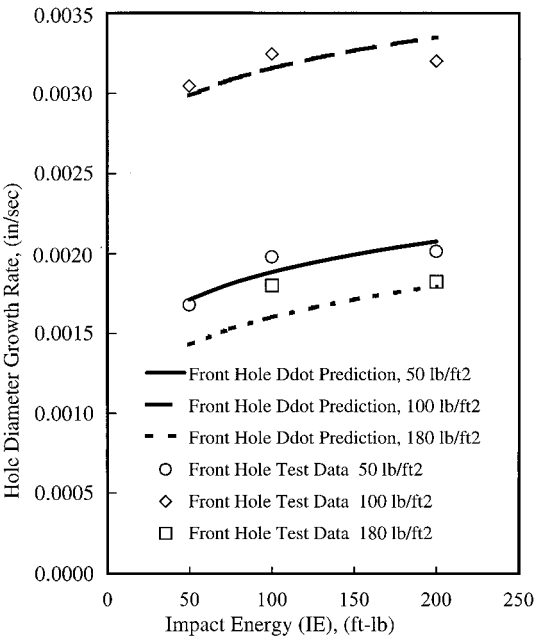

Fig. 14 Comparisons of test data and predictions for front hole growth rate (impact energy).

Figures 13–16 illustrate the effects of impact energy and pressure on hole growth. As expected with increasing impact energy, the hole growth rate increases as a result of coating and substrate damage. As the arcjet test pressure was increased from 50 to 180 lb/ft^2, hole growth increased as the pressure changed from 50 to 100 lb/ft^2, but then decreased at a pressure of 180 lb/ft^2. This reduction in hole growth is a result of a passive glassy layer (SiO_2) being formed on the carbon surface because the carbon substrate has been impregnated with TEOS as part of the RCC oxidation protection system.

Error Analysis

Arcjet test conditions were established by measuring the temperature of an undamaged specimen with a laser pyrometer's readings that have repeatedly agreed from within −1.2 to +0.5% of its readings with imbedded thermocouples in RCC calibration specimens.[5]

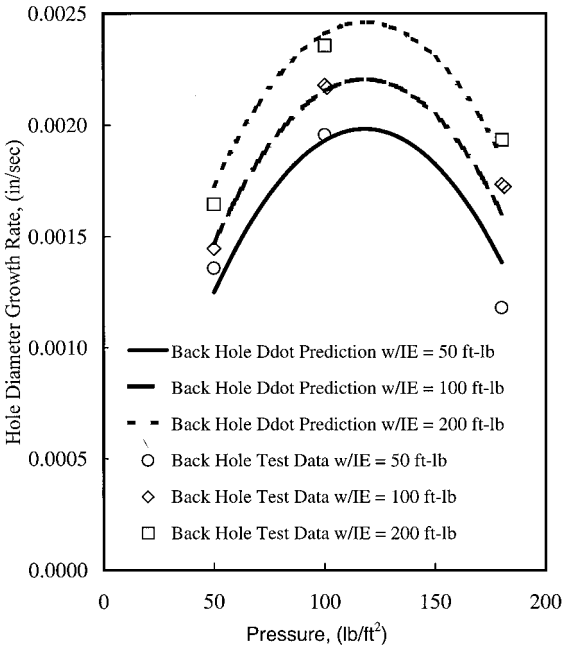

Fig. 15 Comparisons of test data and predictions for back hole growth rate (pressure).

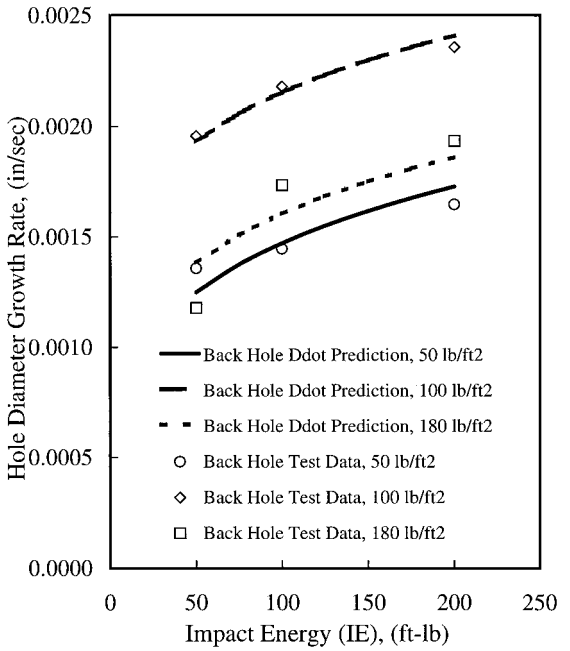

Fig. 16 Comparisons of test data and predictions for back hole growth rate (impact energy).

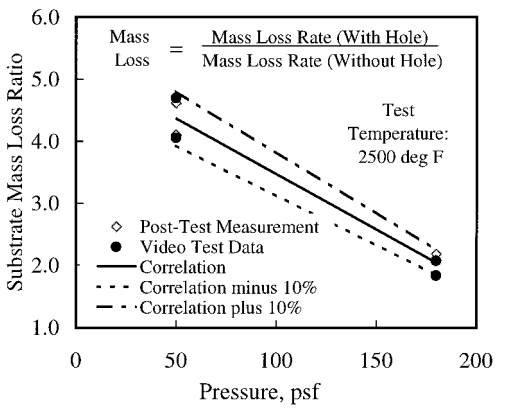

Fig. 17 RCC substrate mass loss ratio with and without an impacted hole.

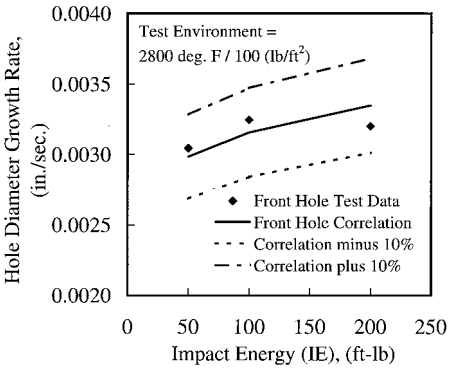

Fig. 18 Impacted RCC front hole growth.

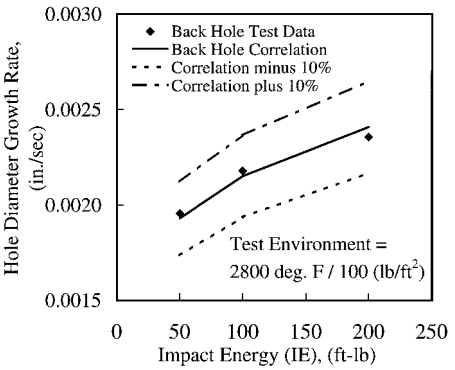

Fig. 19 Impacted RCC back hole growth.

The presence of impact damage in the test specimen results in an increased temperature in the local impact area; however, no changes in the test conditions were made, and all tests were conducted using the calibrated test conditions of a nonimpacted test specimen.

The hole growth measurements made by the JSC IS&AG indicated a minimum uncertainty of 0.01-in.-diam measurements for the inner hole edge and 0.03–0.05 in. for the outer edge diameter. These uncertainties represent an error of approximately 1–7% in the final hole diameter as measured from the videotapes.

Typical comparisons of the regression lines with the test data for ±10% errors are shown in Figs. 17–19, and the complete comparisons for all of the test data are provided in Ref. 5. The correlations are in good agreement with the limited test data and the error analysis indicates that the correlations can be used with confidence in predicting the growth of impacted holes in RCC for flight conditions.

Application to Flight

A flight simulation was performed using the correlations developed, as well as the following methodology. The entry flight is divided into four periods. The first period is from the beginning of the entry to when the RCC temperature reaches 900°F. There is no oxidation for temperatures below 900°F. For the second period (900–2800°F), there is no coating oxidation; however, hole growth occurs due to the oxidation of the exposed RCC substrate. The substrate oxidation rates were used with the test data shown in Table 3 to predict substrate hole growth. The third period, from the time when the temperature is above 2800°F, the hole growth is calculated by the coating correlations developed from the 2800°F test data (Table 4). In the final period, for temperatures below 2800°F to orbiter touchdown, limited substrate oxidation occurs.

Assessment of an entry environment using the methodology developed begins with thermal entry analysis for the entire RCC leading-edge subsystem. For this example, the International Space Station (ISS) shuttle mission (case R ISS, 233 K, 57-deg inclination, forward c.g.) entry trajectory was chosen. Presented in Fig. 20 are the temperature histories that represent the entire wing leading edge. For this assessment of the RCC wing leading-edge areas where temperatures are predicted to be below 2800°F, the hole growth is not expected to expand beyond the coating damage surrounding

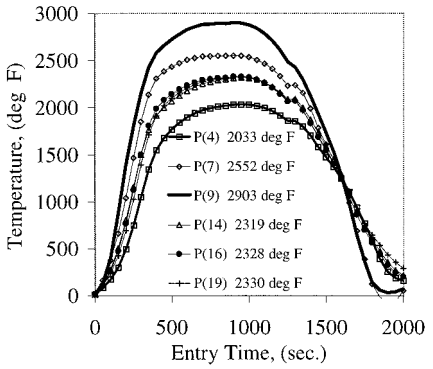

Fig. 20 Temperature histories for the stagnation areas of the wing leading-edge panels 4, 7, 9, 14, 16, and 19 for the ISS mission case R (233 K, 57-deg inclination entry trajectory).

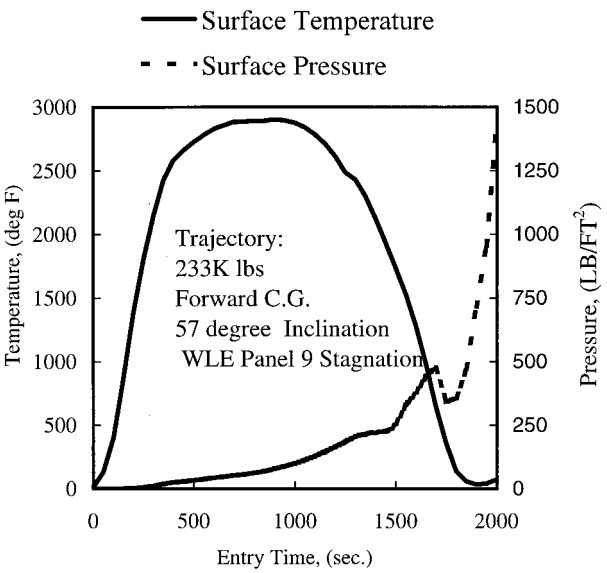

Fig. 21 Temperature and pressure profiles of a typical reentry trajectory.

the impacted hole. An examination of the RCC temperatures reveal that only panels 8, 9, and 10 stagnation areas would experience entry temperatures above 2800°F where major coating erosion would be predicted. The entry environment for panel 9 stagnation area is presented in Fig. 21.

The assessment of the impact damage area of the wing leading-edge panel requires the prediction of the expected hole growth history. This hole growth history is used to evaluate the consequences of the potential damage effects to orbiter structure. For this example a 0.250-in.-diam hole resulting from an MOD impact was assumed. Figure 22 presents the predicted hole growth history for the ISS case R trajectory. The back hole growth rate is used to calculate the hot gas influx into the wing leading-edge cavity for assessing wing spar insulation and structural damage. Final hole diameter growths of 1.5 and 1.15 in., respectively, for the front and back surfaces are predicted.

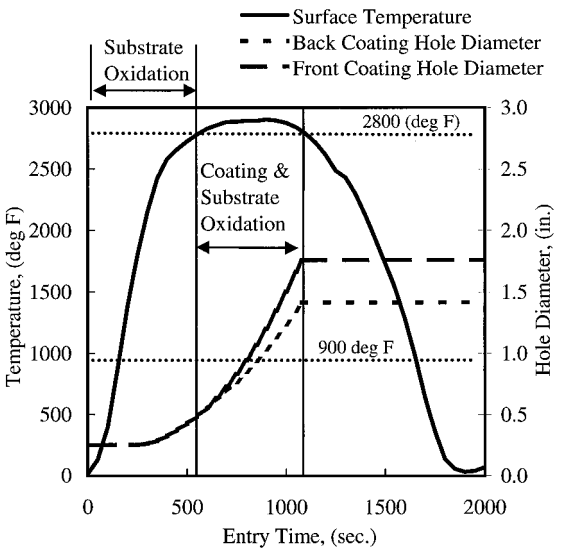

Fig. 22 RCC hole growth history for ISS case R entry trajectory.

Conclusion

This paper presented results from arcjet tests conducted on HVI RCC test specimens and hole growth rates measured with video techniques and posttest examinations. Included were correlations developed for both front-face and back-face mass loss as a function of HVI energy, pressures, and two test temperatures, 2500 and 2800°F. An assessment of a typical entry with an assumed impact damage to estimate hole growth was included. These correlations, along with the probabilities of impact damage, can be used to assess MOD impacts on the orbiter RCC and hot gas flux though an enlarging hole with resultant impingement on the internal insulation components.

Acknowledgments

The authors wish to express their appreciation to Eric Christensen and Frankel Lyons of the NASA Johnson Space Center (JSC) Hypervelocity Impact Technology Facility and J. D. Milhoan of the NASA JSC Atmospheric Reentry Materials and Structures Evaluation Facility for participating and contributing to this work.

References

[1]Curry, D. M., Scott, H. C., and Webster, C. N., "Material Characteristics of Space Shuttle Reinforced Carbon–Carbon," *Proceedings of 24th National SAMPE Symposium*, Vol. 24, Book 2, Society for the Advancement of Material and Process Engineering, Covina, CA, 1979, pp. 1524–1531.

[2]Dotts, R. L., Curry, D. M., and Tillian, D. J., "Orbiter Thermal Protection System," NASA CP-2342, Pt. 2, 1983, pp. 1062–1081.

[3]Lyons, F., "Hypervelocity Impact Testing of Reinforced Carbon–Carbon (RCC)," JSC 28398, May 1998.

[4]Williams, S. D., Curry, D. M., Chao, D. C., and Pham, V. T., "Ablation Analysis of the Shuttle Orbiter Oxidation Protected Reinforced Carbon–Carbon," *Journal of Thermophysics and Heat Transfer*, Vol. 9, No. 3, 1995, pp. 478–485.

[5]Curry, D. M., Norman, I., Chao, D. C., and Pham, V. T., "Oxidation of Hypervelocity Impacted Reinforced Carbon–Carbon," NASA TP-1999-209760, March 2000.

M. Torres
Associate Editor